NASA TECHNICAL
MEMORANDUM

NASA TM X-53397
February 21, 1966

NASA TM X-53397

GPO PRICE $ _____

CFSTI PRICE(S) $ _____

Hard copy (HC) 3.00

Microfiche (MF) .65

ff 653 July 65

# THE ALLEVIATION OF AERODYNAMIC LOADS ON RIGID SPACE VEHICLES

by MARIO H. RHEINFURTH
Aero-Astrodynamics Laboratory



NASA

*George C. Marshall*
*Space Flight Center,*
*Huntsville, Alabama*

TECHNICAL MEMORANDUM X-53397

# THE ALLEVIATION OF AERODYNAMIC LOADS ON RIGID SPACE VEHICLES

By

Mario H. Rheinfurth

George C. Marshall Space Flight Center

Huntsville, Alabama

## ABSTRACT

A necessary condition for the successful flight of a space vehicle through atmospheric disturbances is to maintain stability at all flight times. It is, however, equally important to keep the responses within the design limits of control deflections and structural loads of the vehicle. The study demonstrates how the control systems engineer can assist in this task by a judicious choice of the control system parameters. To this effect, several typical control modes are analyzed for some basic wind profiles. The extent to which a reduction of aerodynamic loads and control excursions can be expected is discussed for various wind, wind shear, and gust conditions. By restricting the analysis to planar and linearized motion of the vehicle, it is possible to derive a set of preliminary design rules, which allows one to predict the relative merits of the discussed control principles when system parameters or wind structure is changed. In addition, the study provides nomograms for the quick determination of gain settings for accelerometer-controlled vehicles if the gain values are given for angle-of-attack control and vice versa.

NASA-GEORGE C. MARSHALL SPACE FLIGHT CENTER

NASA - GEORGE C. MARSHALL SPACE FLIGHT CENTER

Technical Memorandum X-53397

# THE ALLEVIATION OF AERODYNAMIC LOADS ON RIGID SPACE VEHICLES

By

Mario H. Rheinfurth

CONTROL THEORY BRANCH
DYNAMICS AND FLIGHT MECHANICS DIVISION
AERO-ASTRODYNAMICS LABORATORY
RESEARCH AND DEVELOPMENT OPERATIONS

TABLE OF CONTENTS

LIST OF ILLUSTRATIONS

## DEFINITION OF SYMBOLS

| Symbol | Definition |
|---|---|
| $F$ | swivel thrust, newton |
| $\bar{g}$ | longitudinal thrust acceleration, m $sec^{-2}$ |
| $I$ | moment of inertia about C.M., kg $m^2$ |
| $k$ | radius of gyration, m |
| $\ell_p$ | distance of center of percussion from C.M. ($\ell_p = k^2/x_E$), m |
| $m$ | vehicle mass, kg |
| $M'$ | aerodynamic moment coefficient, newton m |
| $N'$ | aerodynamic normal force coefficient, newton |
| $T$ | total thrust minus drag, newton |
| $V$ | velocity in standard flight direction, m $sec^{-1}$ |
| $v_\xi$ | longitudinal vehicle velocity, m $sec^{-1}$ |
| $v_\eta$ | normal vehicle velocity, m $sec^{-1}$ |
| $v_\parallel$ | longitudinal relative air velocity, m $sec^{-1}$ |
| $v_\perp$ | normal relative air velocity, m $sec^{-1}$ |
| $w$ | wind velocity normal to standard flight path, m $sec^{-1}$ |
| $x$ | abscissa of space-fixed reference frame, m |
| $x_E$ | location of swivel point relative to C.M., m |
| $x_D$ | location of displacement sensor relative to C.M., m |
| $x_V$ | location of velocity sensor relative to C. M., m |
| $x_A$ | location of accelerometer relative to C.M., m |
| $y$ | ordinate of space-fixed reference frame, m |

DEFINITION OF SYMBOLS (Continued)

| Symbol | Definition |
|---|---|
| $\alpha$ | angle of attack |
| $\beta$ | swivel engine deflection |
| $\gamma$ | drift angle ($\dot{y}/V$) |
| $\zeta_c$ | critical damping of control mode |
| $\xi$ | abscissa of body-fixed reference frame, m |
| $\eta$ | ordinate of body-fixed reference frame, m |
| $\varphi$ | attitude angle of vehicle |
| $\omega_c$ | control frequency, $sec^{-1}$ |

(Other symbols and abbreviations are explained in the text.)

TECHNICAL MEMORANDUM X-53397

# THE ALLEVIATION OF AERODYNAMIC LOADS ON RIGID SPACE VEHICLES


## SUMMARY

A necessary condition for the successful flight of a space vehicle through atmospheric disturbances is to maintain stability at all flight times. It is, however, equally important to keep the responses within the design limits of control deflections and structural loads of the vehicle. The study demonstrates how the control systems engineer can assist in this task by a judicious choice of the control system parameters. To this effect, several typical control modes are analyzed for some basic wind profiles. The extent to which a reduction of aerodynamic loads and control excursions can be expected is discussed for various wind, wind shear, and gust conditions. By restricting the analysis to planar and linearized motion of the vehicle, it is possible to derive a set of preliminary design rules, which allows one to predict the relative merits of the discussed control principles when system parameters or wind structure is changed. In addition, the study provides nomograms for quick determination of gain settings for accelerometer-controlled vehicles if the gain values are given for angle-of-attack control and vice versa.


## I. INTRODUCTION

Stability of a space vehicle is attained by proper control of the thrust vector, employing jet tabs or swivel engines. Besides the stability requirement, it is also important to keep the responses caused by atmospheric disturbances within the design limits of the control deflections and the structural loads of the vehicle. This problem is solved in two ways. One is the proper design of the vehicle configuration such that aerodynamic lift and moment coefficients are minimized. The other is the selection of a control mode which provides load relief during the period of flight where aerodynamic disturbances become severe. The possibility and extent of reducing these aerodynamic loads by this second approach are discussed in this report. This study is aimed at establishing general criteria for the prediction of trends under changes of system parameters and wind characteristics. Because of the complexity of the actual system, this necessitates the introduction of several simplifying assumptions. Accordingly, the equations of motion are linearized, and effects of bending, sloshing, inertia, and compliance of the swivel engines are omitted. The motion of the vehicle is restricted

to the yaw plane, and the system is considered to be time-invariant; this restricts the analysis to short time intervals of the flight. The effect of gravity in the yaw plane is neglected. Furthermore, the control equation is assumed to be linear, omitting actuator lags and control filters, and all sensing elements are assumed to be ideal with a transfer function of unity. Although these assumptions at first appear to be very restrictive, it has been proven that such a simplified analysis still preserves the essential features of the space vehicle behavior and provides satisfactory data for preliminary control system design.

The author would like to thank Mr. William D. Clarke for helpful and stimulating discussions during the preparation of this study.

## II. EQUATIONS OF MOTION

In the following analysis, the equations of motion will be derived both in a space-fixed and a body-fixed coordinate system. The reason for this is to show how the necessary linearization of the equations of motion will result in notable differences with respect to the stability and response of the system.

### A. Space-Fixed Coordinate System

The space-fixed coordinate system has its origin at the undisturbed position of the center of mass of the vehicle (Figure 1). The equation of the lateral translation is obtained by summing all forces in the space-fixed y-direction, which yields

$$m\ddot{y} = (T - F) \sin \varphi + F \sin (\varphi + \beta) + N'\alpha \cos \varphi. \qquad (1)$$

The equation of rotation is obtained by summing all moments, which yields

$$I\ddot{\varphi} = - Fx_E \sin \beta - M'\alpha. \qquad (2)$$

The numerical value of the aerodynamic moment coefficient is chosen to be positive for an aerodynamically stable vehicle. The linearization of the equations of motion requires two conditions to hold: the rotational motion $\varphi$ and the engine deflection $\beta$ have to be small.

With these assumptions, the equations of motion can be linearized in the form

$$m\ddot{y} = T\varphi + F\beta + N'\alpha \tag{3}$$

$$I\ddot{\varphi} = - Fx_E\beta - M'\alpha. \tag{4}$$

The angle of attack $\alpha$ in the above equations is defined as

$$\operatorname{tg} \alpha = \frac{v_\perp}{v_\parallel}, \tag{5}$$

where $v_\perp$ and $v_\parallel$ are the relative air velocities perpendicular and parallel to the longitudinal vehicle axis. They can be expressed in terms of space-fixed velocities as

$$v_\perp = V \sin \varphi - \dot{y} \cos \varphi + w \cos \varphi \tag{6}$$

and

$$v_\parallel = V \cos \varphi + \dot{y} \sin \varphi - w \sin \varphi. \tag{7}$$

Inserting equations (6) and (7) in (5) yields the expression of the angle of attack in the form

$$\operatorname{tg}(\alpha - \varphi) = \frac{w - \dot{y}}{V}. \tag{8}$$

This expression can be linearized by restriction to small angle-of-attack values such that

$$\alpha = \varphi + \frac{w - \dot{y}}{V}. \tag{9}$$

B. Body-Fixed Coordinate System

The body-fixed coordinate system has its origin at the center of mass of the vehicle and its abscissa coincides with the longitudinal vehicle axis (Figure 1).

Summing all forces normal to the vehicle yields

$$m\ddot{\eta} = F \sin \beta + N'\alpha, \tag{10}$$

whereas the equation for the rotational mode remains unchanged, i.e.,

$$I\ddot{\varphi} = - Fx_E \sin \beta - M'\alpha. \tag{11}$$

The linearization of the above equations of motion requires now only the restriction to small engine deflections.

$$m\ddot{\eta} = F\beta + N'\alpha \tag{12}$$

$$I\ddot{\varphi} = - Fx_E\beta - M'\alpha. \tag{13}$$

Since the condition under which the equations of motion were linearized are less severe in the body-fixed reference frame, we expect this set of equations to give a better description of the actual behavior of the system than the set of equations of the space-fixed reference frame.

It remains to express the angle-of-attack relation (5) in terms of body-fixed coordinates. This is accomplished by using the kinematical relation

$$\ddot{\eta} = \dot{v}_\eta - \dot{\varphi} v_\xi, \tag{14}$$

which can be directly integrated by observing that

$$v_\xi = - V \cos \varphi. \qquad (V = \text{const.}) \tag{15}$$

This gives the normal vehicle velocity as

$$v_\eta = \dot{\eta} - V \sin \varphi. \tag{16}$$

The corresponding relative air velocities are, therefore, given by

$$v_\perp = V \sin \varphi - \dot{\eta} + w \cos \varphi \tag{17}$$

and

$$v_\parallel = V \cos \varphi - w \sin \varphi. \tag{18}$$

From this follows the expression of the angle of attack in terms of body-fixed coordinates as

$$\operatorname{tg}(\alpha - \varphi) = \frac{w - \dot{\eta} \cos \alpha / \cos(\alpha - \varphi)}{V}. \tag{19}$$

This expression can be linearized by restriction to small rotational angles and small angles of attack; this yields

$$\alpha = \varphi + \frac{w - \dot{\eta}}{V}. \tag{20}$$

## III. CONTROL EQUATION

It now remains to establish the law for controlling the motion of the vehicle. To this effect, we employ a linear feedback control system which establishes a linear relationship between the engine deflection (control vector) and the state variables of the system in the form

$$\beta = a_0\varphi_0 + a_1\dot{\varphi}_0 + a_2\ddot{\varphi}_0 + g_0\eta_0 + g_1\dot{\eta}_0 + g_2\ddot{\eta}_0. \tag{21}$$

The coefficients $a_i$ and $g_i (i = 0,1,2)$ represent the gain values of the various transducers (attitude gyro, rate gyro, accelerometer, etc.) which monitor the motion of the vehicle. The variables $\varphi_o$, $\dot{\varphi}_o$, etc., represent the corresponding output signals. The use of higher derivatives in the control law for more rapid response will in most cases not be necessary. They are, in fact, undesirable because their implementation will cause rather noisy output signals.

Within the accuracy requirements of the subsequent analysis, it is justified to set the output signals monitoring the angular motion of the vehicle equal to their corresponding actual state variables; i.e.,

$$\varphi_o = \varphi, \quad \dot{\varphi}_o = \dot{\varphi}, \quad \ddot{\varphi}_o = \ddot{\varphi}. \tag{22}$$

The output signals of the transducers monitoring the lateral motion, however, depend on their location along the longitudinal vehicle axis. For body-fixed sensors, we can obtain their output signals in terms of state variables (and their time integrals) by using the fundamental relation as given by equations (3) and (12):

$$\ddot{\eta} = \ddot{y} - \bar{g}\varphi. \tag{23}$$

We obtain

$$\ddot{\eta}_o = \ddot{\eta} - x_A\ddot{\varphi} = \ddot{y} - \bar{g}\varphi - x_A\ddot{\varphi} \tag{24a}$$

$$\dot{\eta}_o = \dot{\eta} - x_V\dot{\varphi} = \dot{y} - \bar{g}\int \varphi dt - x_V\dot{\varphi} \tag{24b}$$

$$\eta = \eta - x_D\varphi = y - \bar{g}\int\int \varphi dt - x_D\varphi. \tag{24c}$$

It should be emphasized at this point, that the quantities $\dot{\eta}$ and $\eta$ in the above equations do not represent the velocity and displacement along the normal missile axis, but are merely the time integrals of the normal vehicle acceleration, $\ddot{\eta}$.

The effect of the integral terms appearing in these equations is often undesirable. They can be compensated for by appropriate integrations of the output signal of the attitude gyro. These terms can also be eliminated by mounting the transducers on the space-fixed stabilized

platform. The gain values associated with such platform-mounted sensors will be designated by $e_i$. In this case, the control equation is written in the form

$$\beta = a_o\varphi + a_1\dot{\varphi} + a_2\ddot{\varphi} + e_o y_o + e_1\dot{y}_o + e_2\ddot{y}_o, \tag{25}$$

where the output signals are given by

$$\ddot{y}_o = \ddot{y} - x_A\ddot{\varphi} \tag{26a}$$

$$\dot{y}_o = \dot{y} - x_V\dot{\varphi} \tag{26b}$$

$$y_o = y - x_D\varphi. \tag{26c}$$

In general, some sensors will be body-mounted; others will be platform-mounted. In each case, the output signals must be expressed in terms of body-fixed or space-fixed coordinates depending on the equations of motion used. The following discussion assumes a body-fixed accelerometer and platform-mounted velocity meter and displacement meter. The control equation, therefore, has the form

$$\beta = a_o\varphi + a_1\dot{\varphi} + a_2\ddot{\varphi} + e_o y_o + e_1\dot{y}_o + g_2\ddot{\eta}_o. \tag{27}$$

Adopting a space-fixed reference frame, we must first express the output signals of the sensors in terms of space-fixed coordinates using the relations (24) and (26); this yields

$$\beta = \bar{a}_o\varphi + \bar{a}_1\dot{\varphi} + \bar{a}_2\ddot{\varphi} + e_o y + e_1\dot{y} + g_2\ddot{y}, \tag{28}$$

where

$$\bar{a}_o = a_o - e_o x_D - g_2\bar{g} \tag{29a}$$

$$\bar{a}_1 = a_1 - e_1 x_V \tag{29b}$$

$$\bar{a}_2 = a_2 - g_2 x_A. \tag{29c}$$

It is desirable to simplify the control equation (28) by eliminating the lateral and angular acceleration terms using the equations of motion (3) and (4) of the space-fixed coordinate system. This yields the control equation in the simplified form

$$\beta = A_o\varphi + A_1\dot{\varphi} + E_o y + E_1\dot{y} + B_o\alpha, \tag{30}$$

with

$$A_o = \frac{mI(a_o - x_D e_o)}{m_o} \qquad E_o = \frac{mI}{m_o} e_o$$

$$A_1 = \frac{mI(a_1 - x_V e_1)}{m_o} \qquad E_1 = \frac{mI}{m_o} e_1 \tag{31}$$

$$B_o = \frac{(N'I + mx_A M')\, g_2 - m\, M' a_2}{m_o}$$

$$m_o = mI + mFx_E a_2 - F(mx_E x_A + I)\, g_2.$$

It is interesting to notice that only the term $B_o$ contains aerodynamic parameters. The above transformation shows that it is possible to replace an accelerometer by an equivalent angle-of-attack meter and vice versa.

Because of the relationships of equation (31), we can assume without loss of generality that the control equation is given in the form (30). The gain value for the equivalent accelerometer in equation (28) is then simply

$$g_2 = \frac{mI\, B_o + m(x_E F\, B_o + M')\, a_2}{IN' + m\, M' x_A + F(I + mx_E x_A)\, B_o}. \tag{32}$$

Substituting an equivalent accelerometer for an angle-of-attack meter can be done with or without resorting to an angular acceleration feedback as indicated by the free parameter $a_2$ in equation (32). The angular acceleration feedback term $a_2$ could be used to compensate for unreasonably high or low values of the accelerometer gain $g_2$. An illustration of such a conversion from angle-of-attack meter to equivalent accelerometer and vice versa is given in the nomograms of Figures 2 through 4 for the Saturn V vehicle at maximum dynamic pressure. In Figure 2, the dependency of the gain values of an equivalent accelerometer is shown with

respect to its location along the longitudinal vehicle axis with the gain value $B_o$ of the angle of attack as parameter and no angular acceleration feedback ($a_2 = 0$). For high gain values of the angle-of-attack meter, locations of the accelerometer in front of the center of mass ($x < 0$) require excessively high accelerometer gains and are therefore to be avoided.

Figures 3 and 4 show similar nomograms employing angular acceleration feedback which results in changes of the gain value of the equivalent accelerometer. The above results could have also been derived using a body-fixed reference frame as long as the arising integral terms are properly compensated for. Such a compensation is necessary when a body-fixed velocity meter and displacement meter are used in a space-fixed reference frame. In the following discussion, it will always be assumed that the proper compensation has been done such that ensuing results and conclusions apply equally well to a body-fixed or space-fixed reference frame.

## IV. SYSTEM STABILITY

The characteristic equation governing system stability in the space-fixed reference frame is obtained by omitting the external disturbance w, assuming a time dependency of $e^{st}$ in equations (7), (8), and (9) and setting the resultant determinant equal to zero. This yields the fourth order polynomial:

$$mIs^4 + \left(\frac{IN'}{V} + \frac{F\,B_o\,I}{V} - FIE_1 + mA_1Fx_E\right) s^3 + \left(\frac{N'\,Fx_E}{V} A_1 - \frac{FM'}{V} A_1 + m\,Fx_E\,B_o + m\,M' - FIE_o + m\,Fx_E A_o\right) s^2 + \left(\frac{N'\,Fx_E}{V} A_o - \frac{FM'}{V} A_o - \frac{TFx_E}{V} B_o - \frac{TM'}{V} - FM'E_1 + N'x_E\,FE_1 + TFx_E\,E_1\right) s + (N'x_E - M' + Tx_E)\,FE_o = 0. \tag{33}$$

To simplify further discussion, we abandon the constraint of the lateral translation by setting $E_o = 0$. As a consequence, the vehicle has lost control over its lateral position. This penalty, however, is not severe, since one can hope to correct for a temporary deviation from the standard flight trajectory at a later flight time. The characteristic equation is now of third order. Two of its roots are, in general, conjugate complex (control roots) having an absolute value which is large compared to the absolute value of the third real root (drift root) of the polynomial. The stability behavior of the rotational mode (control mode) can, therefore, be approximately analyzed by the first three terms of the polynomial (33)

$$s^2 + \left(\frac{N'}{mV} + \frac{FB_o}{mV} - \frac{FE_1}{m} + \frac{A_1 Fx_E}{I}\right)s + \left\{\frac{F}{V}\left(\frac{N'x_E - M'}{mI}\right)A_1 + \frac{Fx_E (A_o + B_o) + M'}{I}\right\} = 0. \tag{34}$$

From equation (34) we can draw several important conclusions. The first concerns the frequency of the rotational mode (control frequency) which is represented by the last term of the above equation. It is affected by both the attitude and angle-of-attack feedback $(A_o + B_o)$. The attitude rate feedback, $A_1$, has the tendency to increase the control frequency. This influence is, however, very small and can be neglected in most practical cases. It is also important to notice the absence of a velocity feedback term, $E_1$, from which we conclude that its influence on the (undamped) control frequency is also negligible. The undamped control frequency can, therefore, be approximated by

$$\omega_c^2 = \frac{Fx_E (A_o + B_o) + M'}{I} . \tag{35}$$

Because of experimental and theoretical uncertainties in the aerodynamic coefficient $M'$ ($< 0$ for unstable configurations), it is common practice to choose the values of $A_o$ and $B_o$ such that the first term of equation (35) becomes predominant in order to guarantee a comfortable stability margin.

The second conclusion concerns the damping of the control mode which is represented by the second term of equation (34). Angle-of-attack feedback ($B_o$) tends to increase the damping of the control mode, whereas velocity feedback ($E_1$) decreases it. However, both of these influences are small in comparison to the attitude rate feedback term, $A_1$, for practically encountered gain values. The aerodynamic damping term in

equation (34) is also very small such that the "control damping" can be approximately written as

$$\zeta_c \approx \frac{A_1 Fx_E}{2I\ \omega_c} = \frac{A_1\ \omega_c}{2(A_o + B_o + M'/Fx_E)}. \tag{36}$$

Dropping all negligible terms in equation (33), we can rewrite it in the form

$$mIs^3 + mA_1\ Fx_E s^2 + \left\{mFx_E\ (A_o + B_o) + m\ M'\right\} s\ + \frac{F(N'x_E - M')}{V} A_o$$

$$- \frac{TFx_E\ B_o}{V} - \frac{TM'}{V} + F(N'x_E - M' + Tx_E)\ E_1 = 0. \tag{37}$$

The stability boundaries of this equation are given as follows:

(a) Static Stability Boundary ($D_o = 0$)

$$B_o = \frac{(N'x_E - M')\ A_o + \{(T + N')\ x_E - M'\}\ \bar{E}_1 - \frac{T}{F} M'}{Tx_E}. \tag{38}$$

(b) Dynamic Stability Boundary ($D_1D_2 = D_oD_3$)

$$B_o = \frac{(N'x_E - M' - \bar{A}_1Fx_E)\ A_o + \{(T + N')\ x_E - M'\}\ \bar{E}_1 - (\frac{T}{F} + \bar{A}_1)\ M'}{(T + \bar{A}_1F)\ x_E}, \tag{39}$$

where $\bar{E}_1 = E_1V$ and $\bar{A}_1 = A_1V/\ell_p$.

The stability boundaries become straight lines in the $B_o/A_o$-plane using $\bar{E}_1$ as a parameter or in the $\bar{E}_1/A_o$-plane using $B_o$ as a parameter. The corresponding stability areas are illustrated for pure angle-of-attack feedback ($\bar{E}_1 = 0$) in Figure 5 and for pure velocity feedback ($B_o = 0$) in Figure 6. Both figures show the stability areas for the system described in a space-fixed as well as in a body-fixed coordinate system. The transition from space-fixed to body-fixed coordinates is readily obtained by setting $T = 0$ in equations (38) and (39). Because of the dominance of the $A_1$-term in equation (39), the dynamic stability line in the $B_o/A_o$-plane has a slope of approximately -45 degrees, and the slope of the dynamic stability line in the $\bar{E}_1/A_o$-plane assumes a rather high (positive) value.

A comparison of the stability behavior of the system shows a remarkable difference between the space-fixed and body-fixed coordinate system regarding the boundaries of static instability. In the space-fixed coordinate system, this static instability occurs if the angle-of-attack feedback gain, $B_o$, is being increased. Physically it represents the gain value of $B_o$ beyond which the vehicle turns its nose into the wind to such a degree that it acquires a negative drift velocity; i.e., the vehicle flies against the wind.

Another point of interest in the stability areas is the zero-crossing of the dynamic stability boundary. This occurs approximately at the value of the angular displacement feedback gain, $A_o$, at which the restoring moment of the swivel engines compensates the overturning aerodynamic moment.

## V. STEADY-STATE RESPONSE

The response of the vehicle is subject to two basic constraints. One is the limitation of the control variable, $\beta$, the other the design limit of the bending moment. For rigid body considerations, as in this discussion, the bending moment can be expressed as a linear combination of the angle-of-attack, $\alpha$, and the control variable, $\beta$, in the form [1]:

$$M(x,t) = M'_{\alpha}(x)\ \alpha(t) + M'_{\beta}(x)\ \beta(t). \qquad (40)$$

The objective of aerodynamic load relief is to reduce this bending moment by a control system design which forces the vehicle to turn into the wind without excessively high excursions of the engine deflection. To investigate the response pattern of the various control modes which we can choose within the stability areas depicted in Figures 5 and 6, we first derive the expression for the steady state response of the system to a unit step input.

This is obtained by setting all time derivatives equal to zero. Since we assume in the following that the guidance term, $E_o$, is omitted, the system is only quasi-stable in its lateral position, y. Therefore, the vehicle assumes in its steady state a constant lateral velocity, $\dot{y}$, when a unit step function is applied and we have to retain all $\dot{y}$-terms in the equations when the steady state responses are obtained for this case.

By introducing the abbreviation

$$C_o = (N'x_E - M')\,A_o - Tx_E\,B_o - \frac{T}{F}M' + (N'x_E - M' + Tx_E)\,\bar{E}_1, \qquad (41)$$

the steady-state response in the space-fixed coordinate system is thus given as

$$(\alpha/\alpha_w)_{ss} = \frac{Tx_E}{C_o}\,\bar{E}_1 \qquad (42)$$

$$(\beta/\alpha_w)_{ss} = \frac{\frac{T}{F}M'}{C_o}\,\bar{E}_1 \qquad (43)$$

$$(\varphi/\alpha_w)_{ss} = -\frac{(N'x_E - M')}{C_o}\,\bar{E}_1 \qquad (44)$$

$$(\dot{y}/V\alpha_w)_{ss} = \frac{(N'x_E - M')\,A_o - Tx_E\,B_o - \frac{T}{F}M'}{C_o}\,. \qquad (45)$$

The next step is to find control modes which exhibit load relief features such that the vehicle turns into the wind in its steady-state response.

A. Gyro Control

This is the simplest control mode which employs attitude and attitude rate feedback only ($\bar{E}_1 = B_o = 0$). It can be readily seen that in this case all steady-state values vanish with the exception of the lateral velocity, $\dot{y}$, which approaches the wind velocity, w. The vehicle starts drifting with the wind, but does not turn into it. A load relief in the above sense is therefore not achieved, although the steady-state bending moment is zero.

B. Velocity-Feedback Control

This control mode employs a velocity-feedback, $\bar{E}_1$, in addition to attitude and attitude-rate feedback. Since $N'x_E > M'$ and $C_o > 0$ for a (statically) stable vehicle, we deduce from equation (44) that the steady-state attitude of the vehicle is negative; this means, according to the adopted sign convention, that the vehicle turns into the wind and that this control mode exhibits the desired load relief feature. In addition, the lateral drift velocity $\dot{y}$ is smaller than the steady-state wind velocity. Since the vehicle does not completely drift with the wind, it stays closer to the nominal flight path. It assumes steady-state values for angle of attack and engine deflection, and therefore has also a steady-state bending moment.

C. Angle-of-Attack Control

This control mode is characterized by an angle-of-attack feedback, $B_o$, in addition to attitude and attitude rate feedback. In general, this control mode will yield the same steady-state values as the gyro control mode. However, there exists an important special case for a feedback signal, $B_o$, such that

$$B_o = \frac{(N'x_E - M')\,A_o - \frac{T}{F}M'}{Tx_E} \,. \tag{46}$$

With this gain value, the steady-state responses of equations (42)-(45) become independent of the velocity-feedback gain, $\bar{E}_1$. They are as follows:

$$(\alpha/\alpha_w)_{DM} = \frac{Tx_E}{N'x_E - M' + Tx_E} \tag{47}$$

$$(\beta/\alpha_w)_{DM} = - \frac{\frac{T}{F} M'}{N' x_E - M' + T x_E} \tag{48}$$

$$(\varphi/\alpha_w)_{DM} = - \frac{N' x_E - M'}{N' x_E - M' + T x_E} \tag{49}$$

$$(\dot{y}/V\alpha_w)_{DM} = 0. \tag{50}$$

This control mode is referred to as "drift-minimum control" [2]. It derives its name from the fact that, in this particular control mode, the steady-state drift velocity vanishes. If the velocity-feedback, $\bar{E}_1$, is zero (pure angle-of-attack control), then the drift velocity, $\dot{y}$, will assume the indeterminate form 0/0. Physically speaking, this means that the steady-state drift velocity is determined by initial conditions and transient motion of the vehicle. Its final value is usually very small in comparison to the steady-state wind velocity. The drift-minimum control mode, therefore, leads to small deviations from the nominal flight path. From equation (49) it can also be seen that the drift-minimum control mode exhibits the desired load relief feature by assuming a negative steady-state attitude. Because of the dual feature of providing minimum drift and load relief, the drift-minimum control mode has been intensively studied in the past [3, 4]. The steady-state bending moment, however, does not vanish.

The drift-minimum condition of equation (46) leads to an operating point which lies on the static stability boundary of the stability area for the space-fixed coordinate system (Figure 5). This means that the drift root of the characteristic polynomial becomes zero. The 45-degree dotted line represents points for which the control frequency remains constant; i.e., $A_o + B_o = \text{const}$. For the space-fixed coordinate system, the drift-minimum condition represents the highest angle-of-attack feedback possible without becoming unstable. Since no instability, however, occurs at this point in the body-fixed coordinate system, it is possible to further increase the angle-of-attack feedback gain. Keeping the control frequency constant, we thus arrive at a point where the attitude feedback gain, $A_o$, equals 0. This control mode is referred to as "load-minimum control." In this control mode, the vehicle turns completely into the wind ($\varphi = - \alpha_w$). All other steady-state values vanish. Therefore, the steady-state bending moment becomes zero, justifying the name given to this particular control mode.

## VI. TRANSIENT RESPONSE

The control mode to be adopted for load alleviation will also strongly depend on the transient behavior of the vehicle, especially how fast the vehicle can be turned into the wind. The effectiveness of the load alleviation is directly proportional to this "turnability" parameter, which is given by the quantity $C_2 = Fx_E/I$. Other factors of importance are the wind, wind shear and turbulence characteristics, and the relative magnitude of the coefficients $M'_\alpha$ and $M'_\beta$ of the bending moment equation (40) at the critical stations of the vehicle.

To gain more insight into the salient features of the various possible control modes and to assess their relative merits or demerits, the response behavior of a Saturn V space vehicle was investigated for the maximum dynamic pressure region. Two basic wind input functions were applied. One is a ramp input, which serves to illustrate the effect of an average wind shear of 0.02 m/sec/m building up to a maximum level of 75 m/sec, the other a step input of the same magnitude demonstrating the effect of a severe gust condition. The feedback gains of the different control modes investigated were set to give a control frequency of 0.15 cps and a critical control damping of 70 percent in each case. All response curves are plotted for both the space-fixed coordinate system (subscript s) and the body-fixed coordinate system (subscript B).

At first the response behavior is shown for a simple gyro control mode in Figures 7 and 8. The attitude remains positive at all times for the ramp input as well as for the step input. The vehicle does not turn into the wind, and no load relief is obtained. The steady-state values gradually drop to zero with the exception of the drift angle $\gamma$ which approaches the wind angle, $\alpha_w$; i.e., the vehicle drifts with the wind. Introducing angle-of-attack feedback in the form of the drift minimum control mode changes the response pattern radically. For the ramp input (Figure 9), the vehicle attitude very rapidly becomes negative; this reduces the angle of attack simultaneously. This reduction of angle of attack can even be achieved with a smaller engine deflection than in the gyro control mode. For such wind input function, the drift minimum control mode would, therefore, also reduce the bending moment in comparison to that of the gyro control mode. Especially conspicuous - at least for the space-fixed coordinate system - is the extremely low drift angle, $\gamma$. The steady state responses approach the values as given in equations (47) through (49). For the step input (Figure 10), the system reacts immediately with a comparatively large transient engine deflection, which causes the vehicle to turn instantly into the wind. This results in a substantial reduction of the angle of attack. After the initial kick, the engine quickly settles down to its steady state value. Because of the high engine excursion, the evaluation of the system response with regard to

the desired load alleviation now becomes more complicated. If the turnability, $C_2$, of the vehicle is high and if the thrust coefficient, $M'_\beta$ of equation (40) does not contribute significantly to the total bending moment, it is possible that the engine deflection stays within its design limit and that the bending moments can be reduced in comparison to those of the gyro control mode. A careful investigation must therefore be made whether or not the predicted wind shear or gust conditions allow a load reduction by using the drift minimum control mode.

Adopting the "load minimum" control mode (Figures 11 and 12) shows that all statements made for the drift minimum control mode apply also for this type of control, but in a stronger sense. Low wind buildups lead to very favorable conditions for load alleviation, whereas high wind shears will lead to even more severe engine deflections than those exhibited for the drift minimum control mode. It is interesting that the already discussed instability of the system which appears in the space-fixed reference frame results in a tumbling of the vehicle. In the body-fixed reference frame, this instability does not exist, and the vehicle merely turns completely into the wind; i.e., $\varphi = -\alpha_w$. Finally Figures 13 and 14 give an example of a velocity feedback control mode. This control mode also causes the vehicle to turn into the wind with a consequent reduction of the bending moment, at least under low wind shear conditions. For high wind shear or gusts, the engine deflections are less severe than in the previously discussed control modes; this makes the velocity feedback an attractive candidate for load reduction under high wind shear and gust conditions. Also, the velocity feedback control mode assists in reducing lateral drift velocities, and should, therefore, be preferred over a reduced angle-of-attack feedback which does not exhibit this feature.

## CONCLUSIONS

The reduction of aerodynamic loads is possible by careful selection of an appropriate control mode under a large class of wind and wind shear conditions. However, the effectiveness of the load reduction depends decisively on the vehicle configuration and the wind shear characteristics of the atmospheric disturbances. If the power level of the atmospheric disturbances is concentrated at high frequencies, the possibility of a load reduction is vastly reduced because of high engine excursions which tend to increase the total bending moments. In this case, improvement can be obtained through various modifications of the discussed control modes by introducing nonlinear and adaptive control techniques. However, preliminary load studies such as those discussed above always have to be supplemented by more refined analyses incorporating the effects of flexibility, sloshing, etc. This, under certain circumstances, can lead to drastic reevaluation, or even rejection, of control modes which had proven to be satisfactory under simplified assumptions.

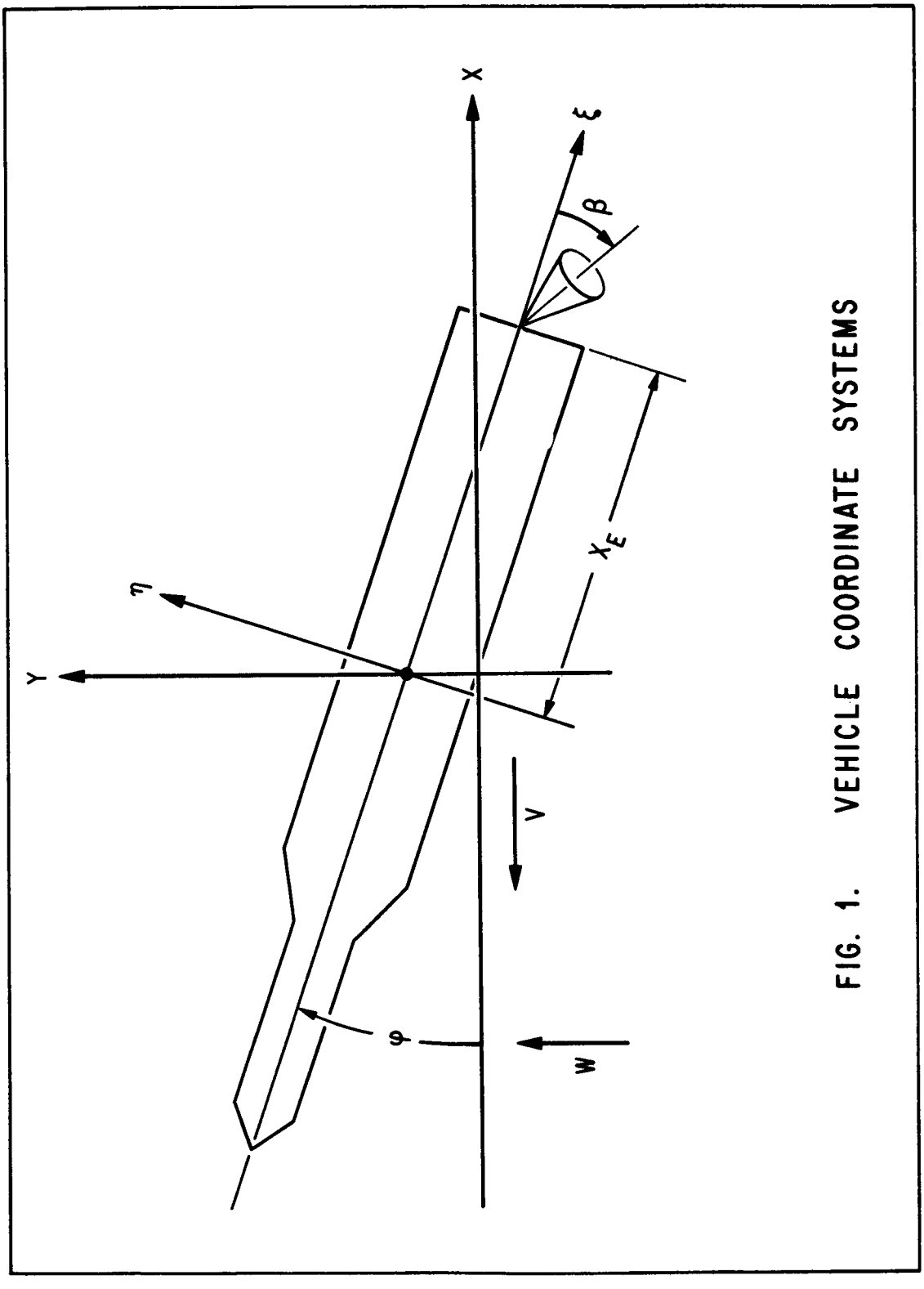


FIG. 1. VEHICLE COORDINATE SYSTEMS

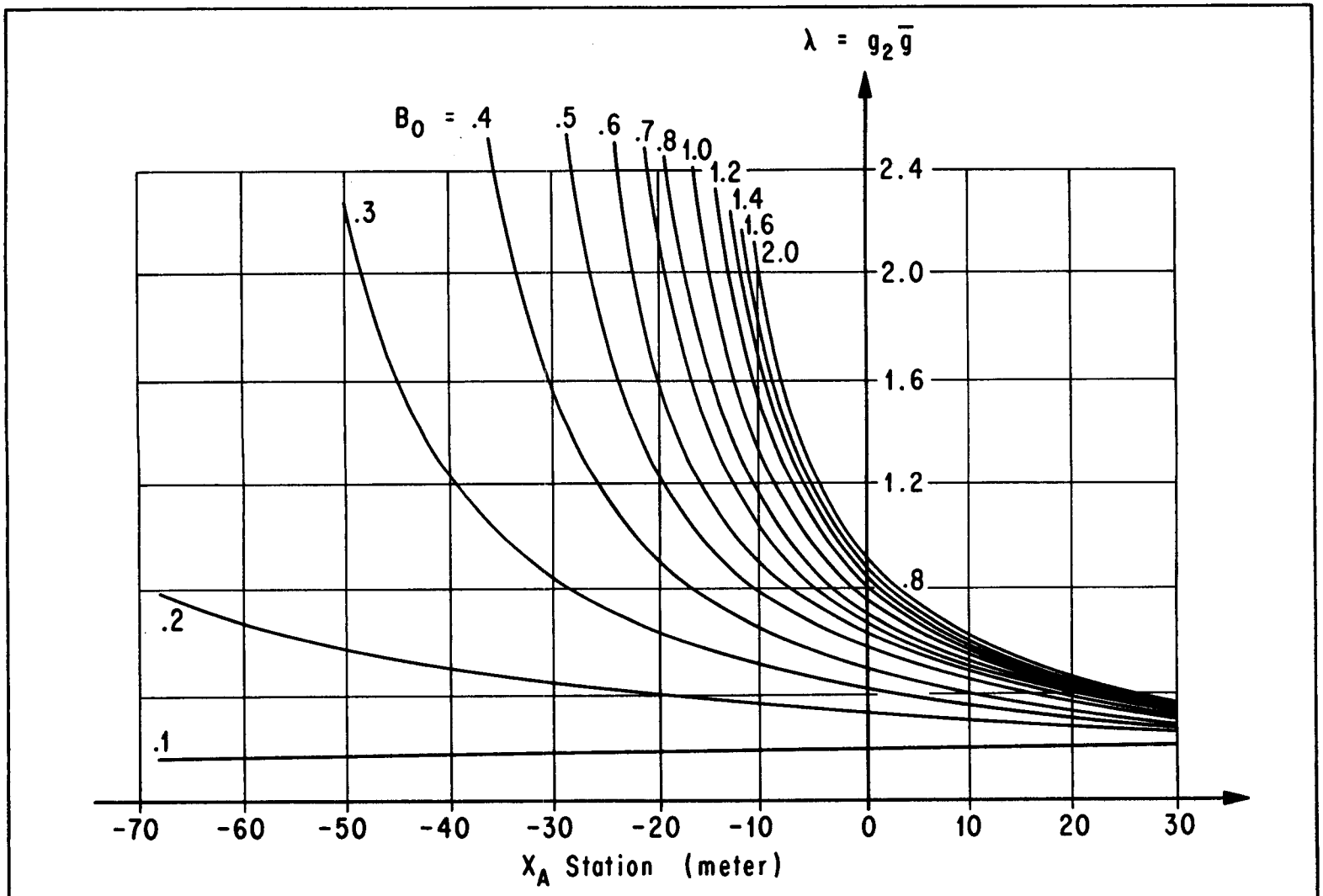


FIG. 2. GAIN VALUES FOR EQUIVALENT ACCELEROMETER ($a_2 = 0$)

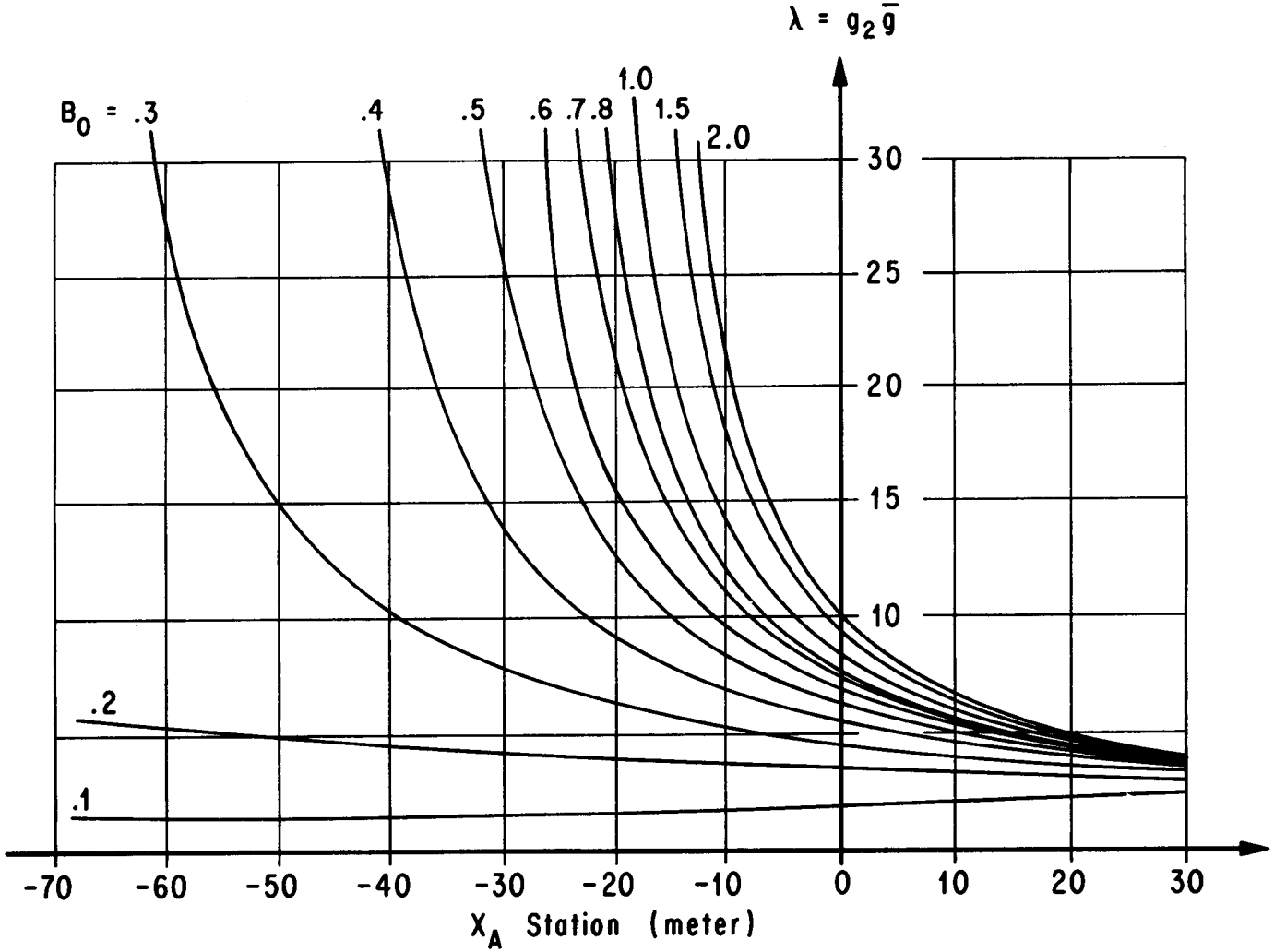


FIG. 3. GAIN VALUES FOR EQUIVALENT ACCELEROMETER ($a_2$ = 1 $SEC^{-2}$)

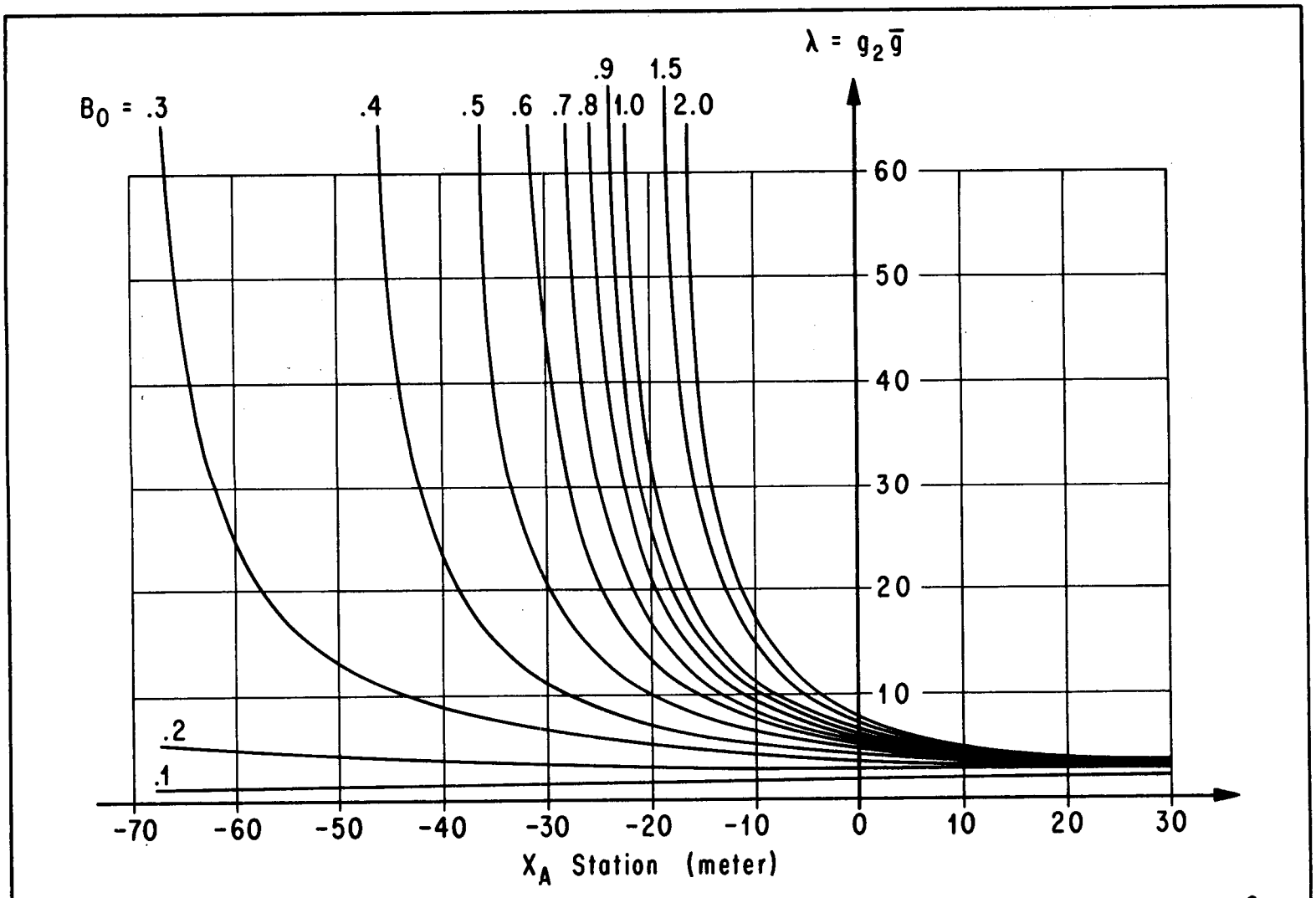


FIG. 4. GAIN VALUES FOR EQUIVALENT ACCELEROMETER ($a_2 = -1$ SEC$^{-2}$)

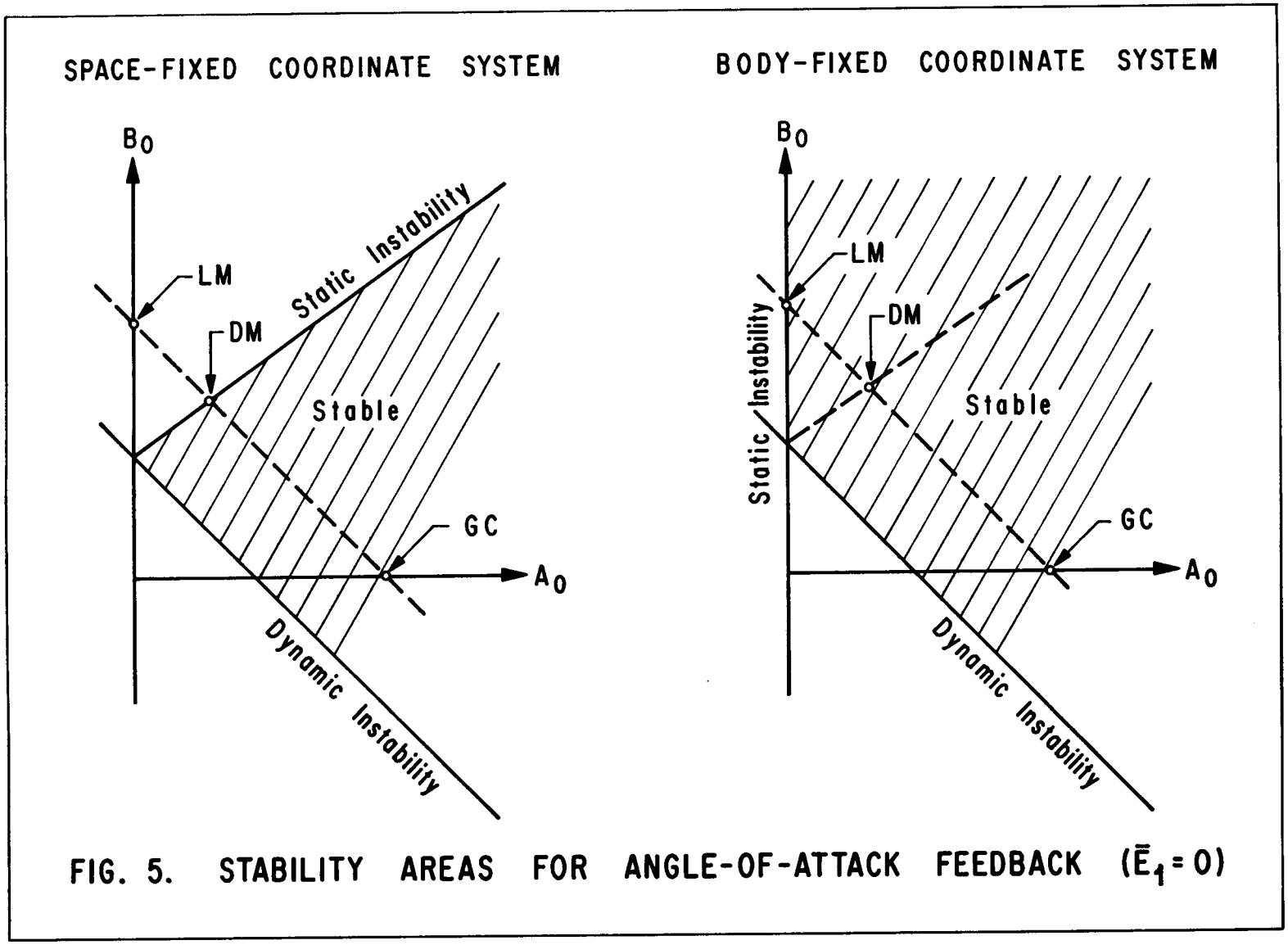


FIG. 5. STABILITY AREAS FOR ANGLE-OF-ATTACK FEEDBACK ($\bar{E}_1 = 0$)

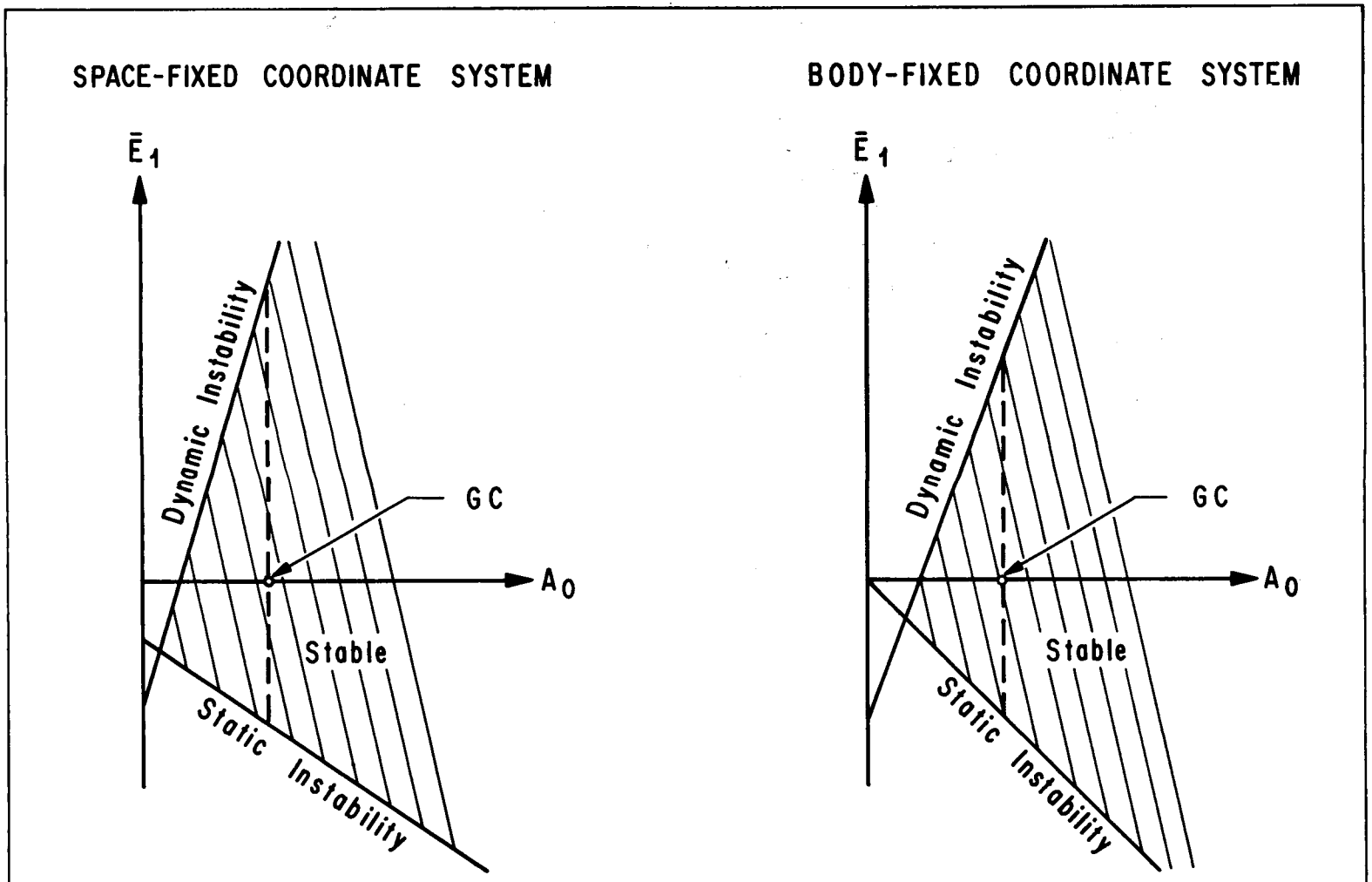


FIG. 6. STABILITY AREAS FOR VELOCITY FEEDBACK ($B_0 = 0$)

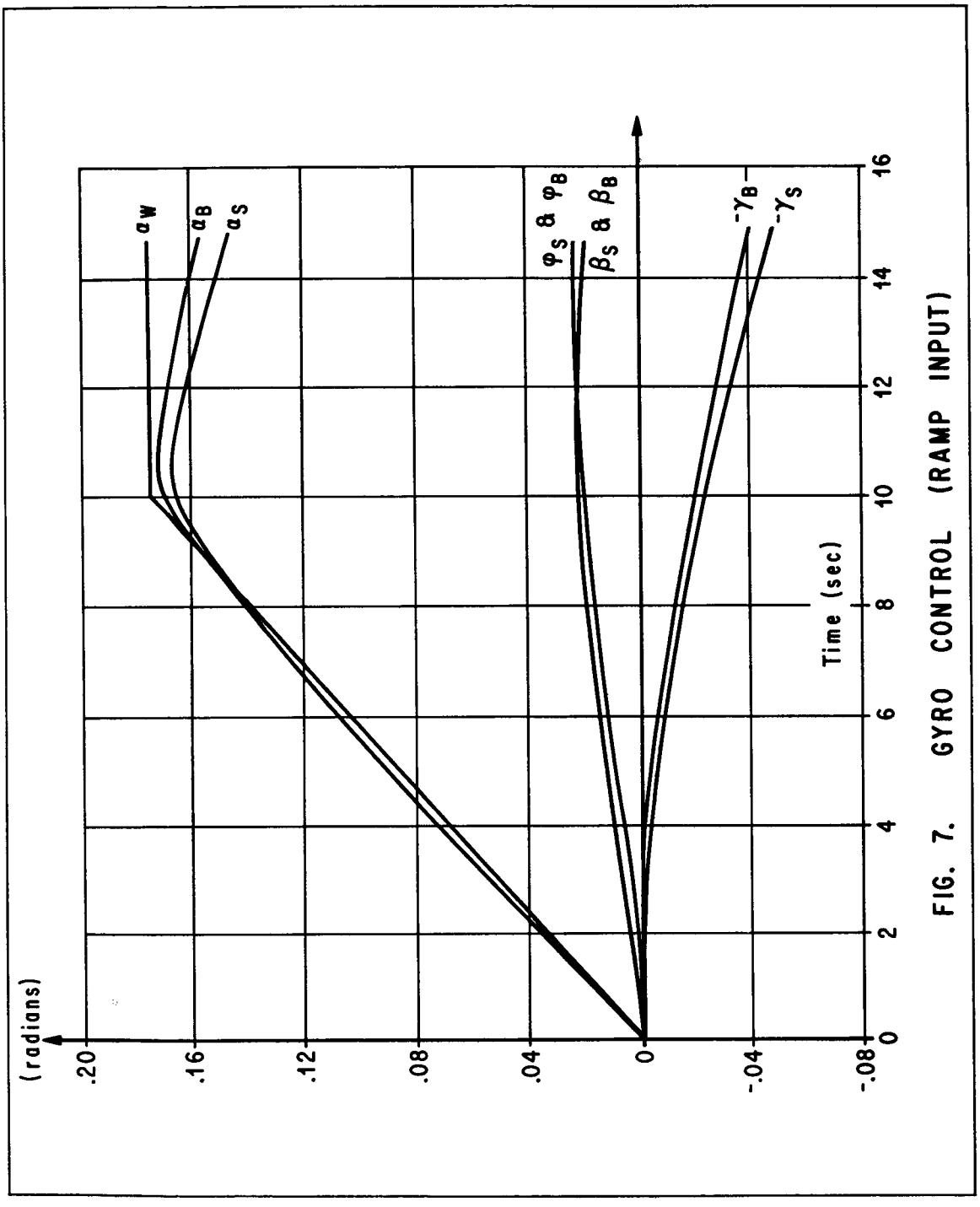


FIG. 7. GYRO CONTROL (RAMP INPUT)

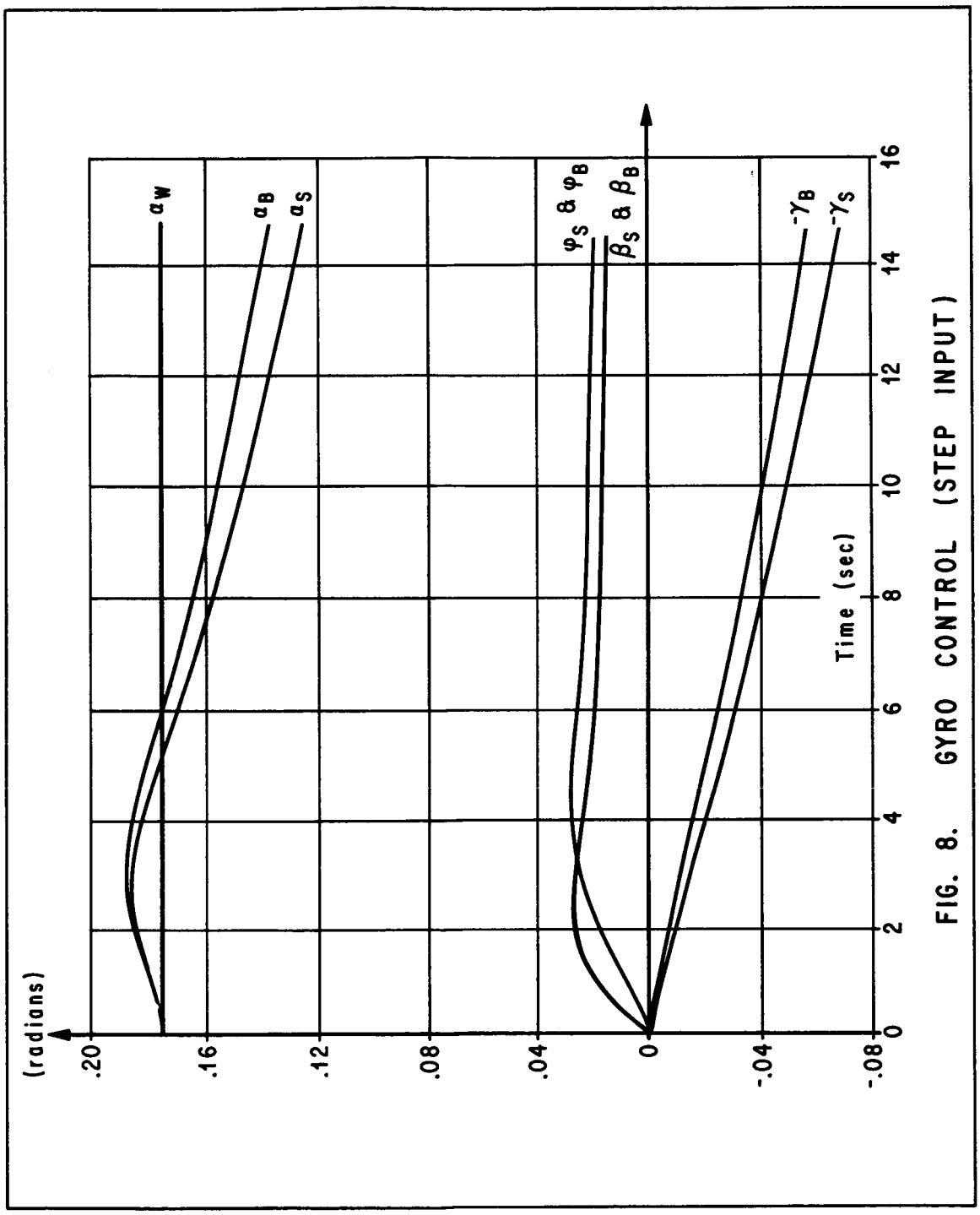


FIG. 8. GYRO CONTROL (STEP INPUT)

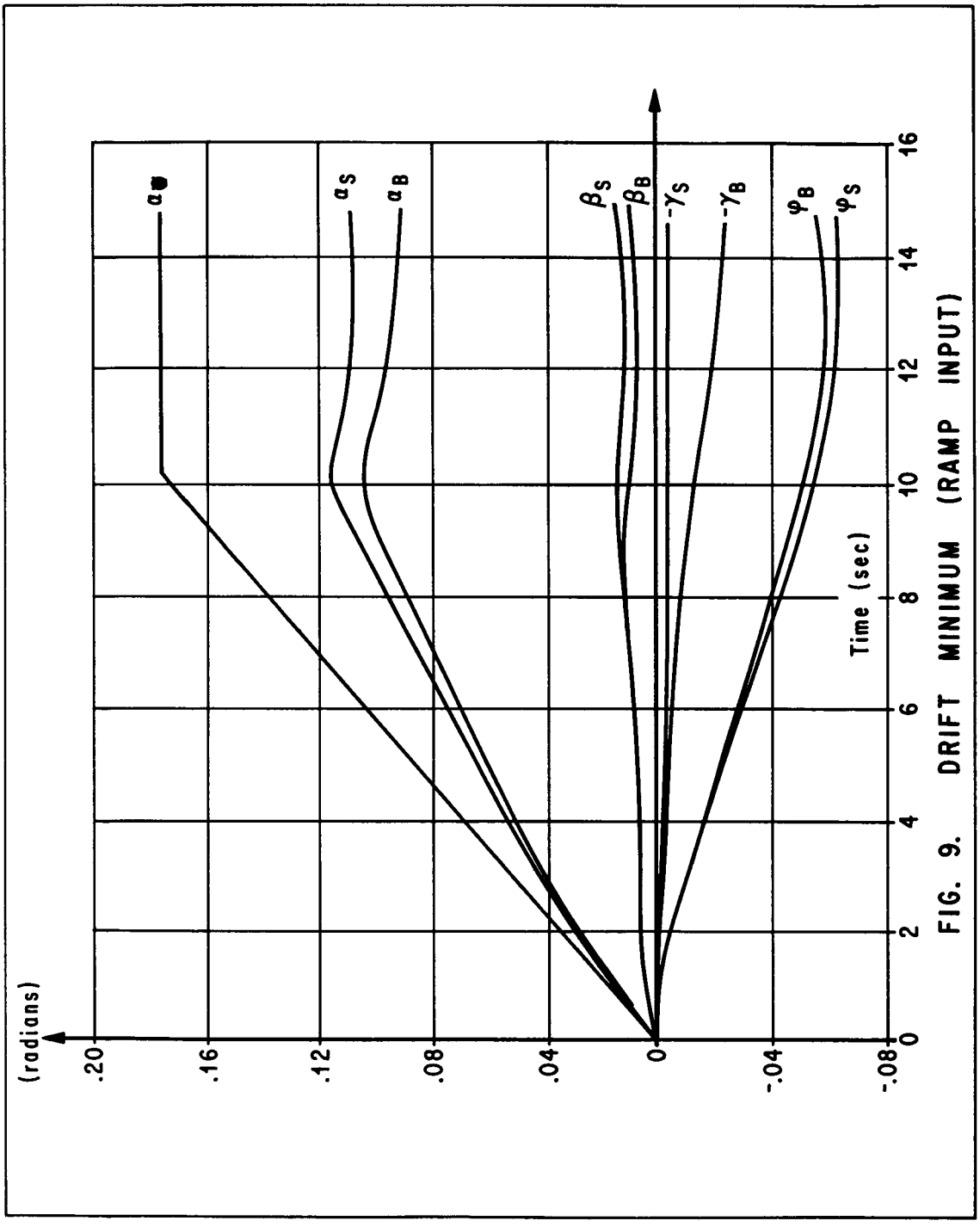


FIG. 9. DRIFT MINIMUM (RAMP INPUT)

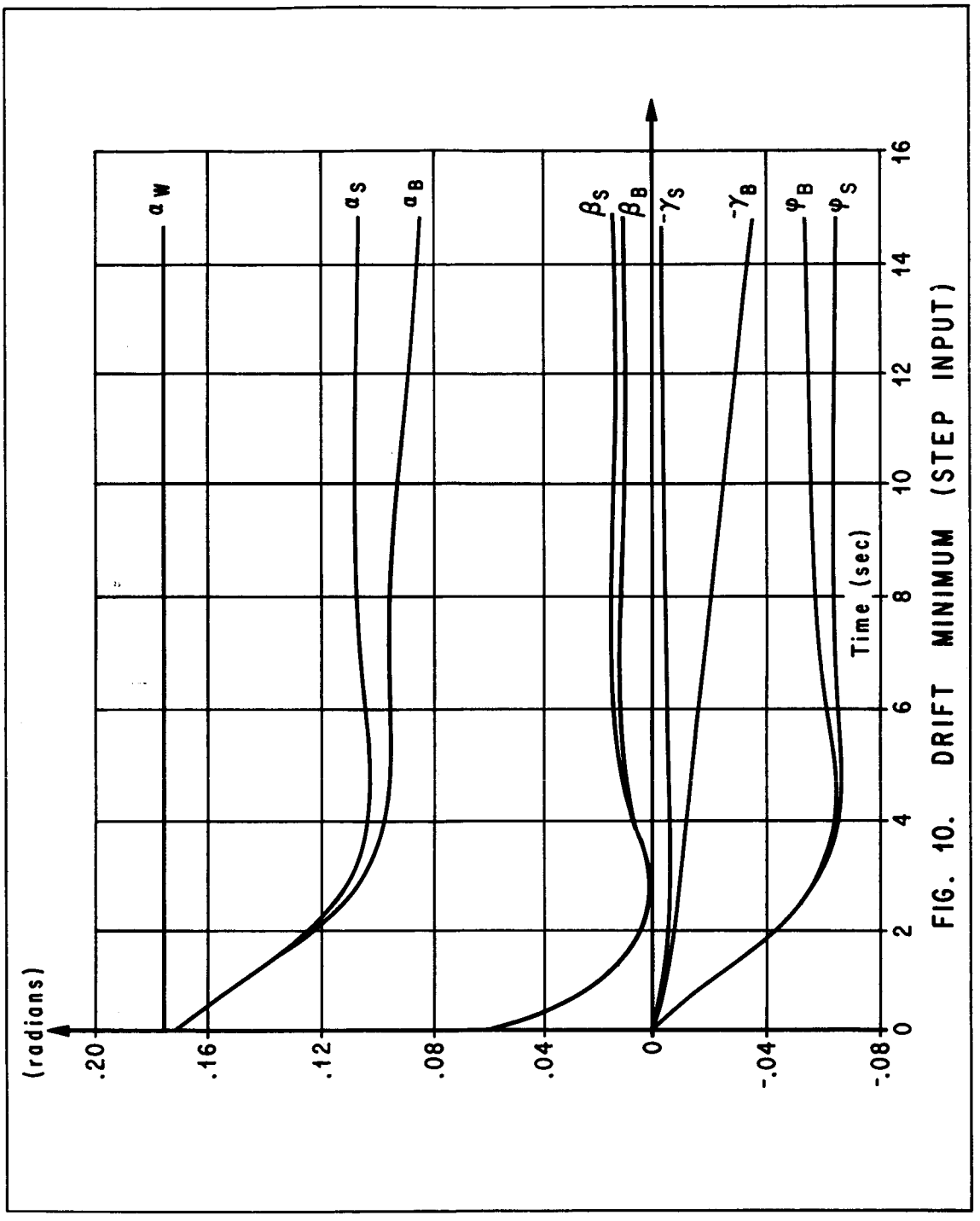


FIG. 10. DRIFT MINIMUM (STEP INPUT)

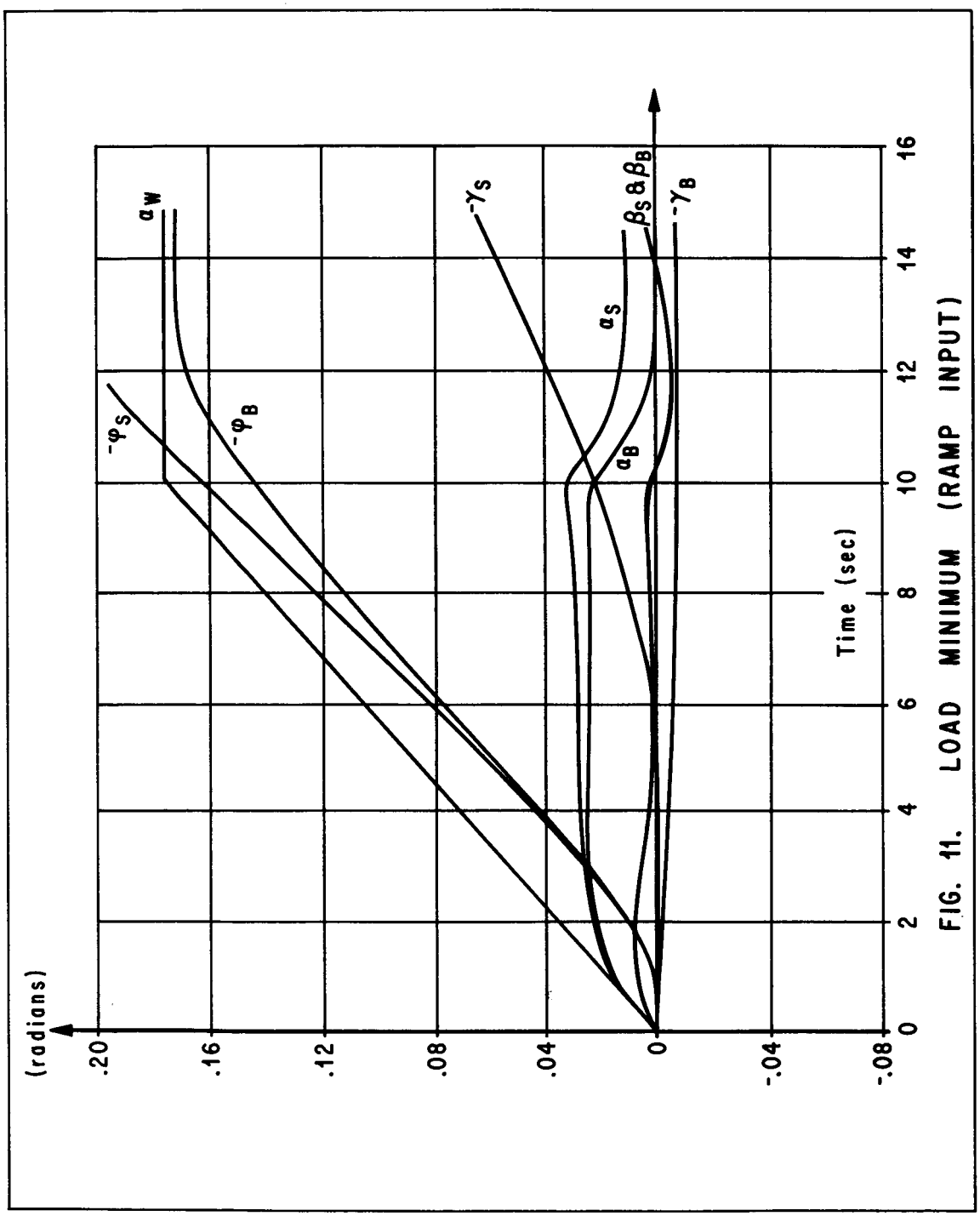


FIG. 11. LOAD MINIMUM (RAMP INPUT)

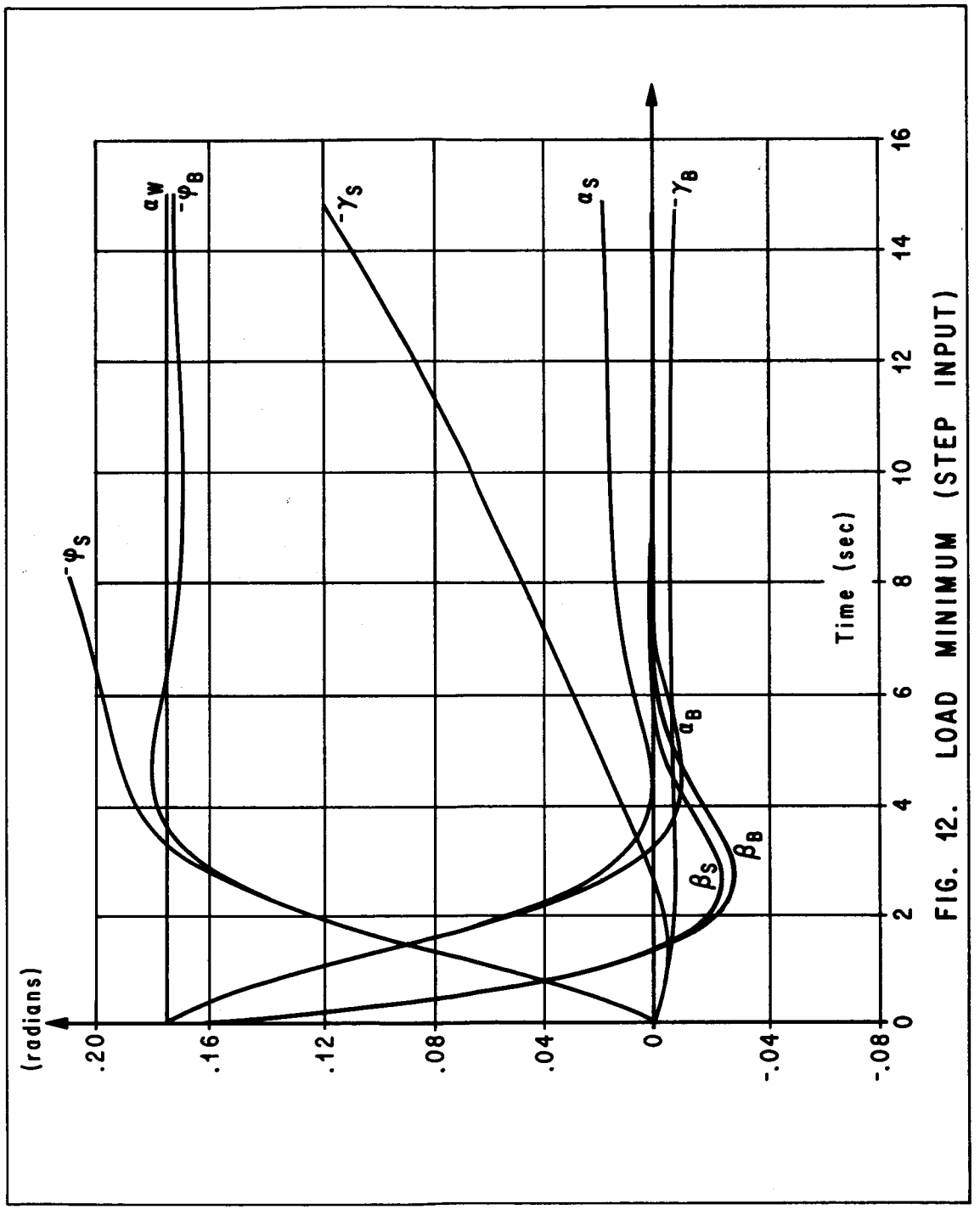


FIG. 12. LOAD MINIMUM (STEP INPUT)

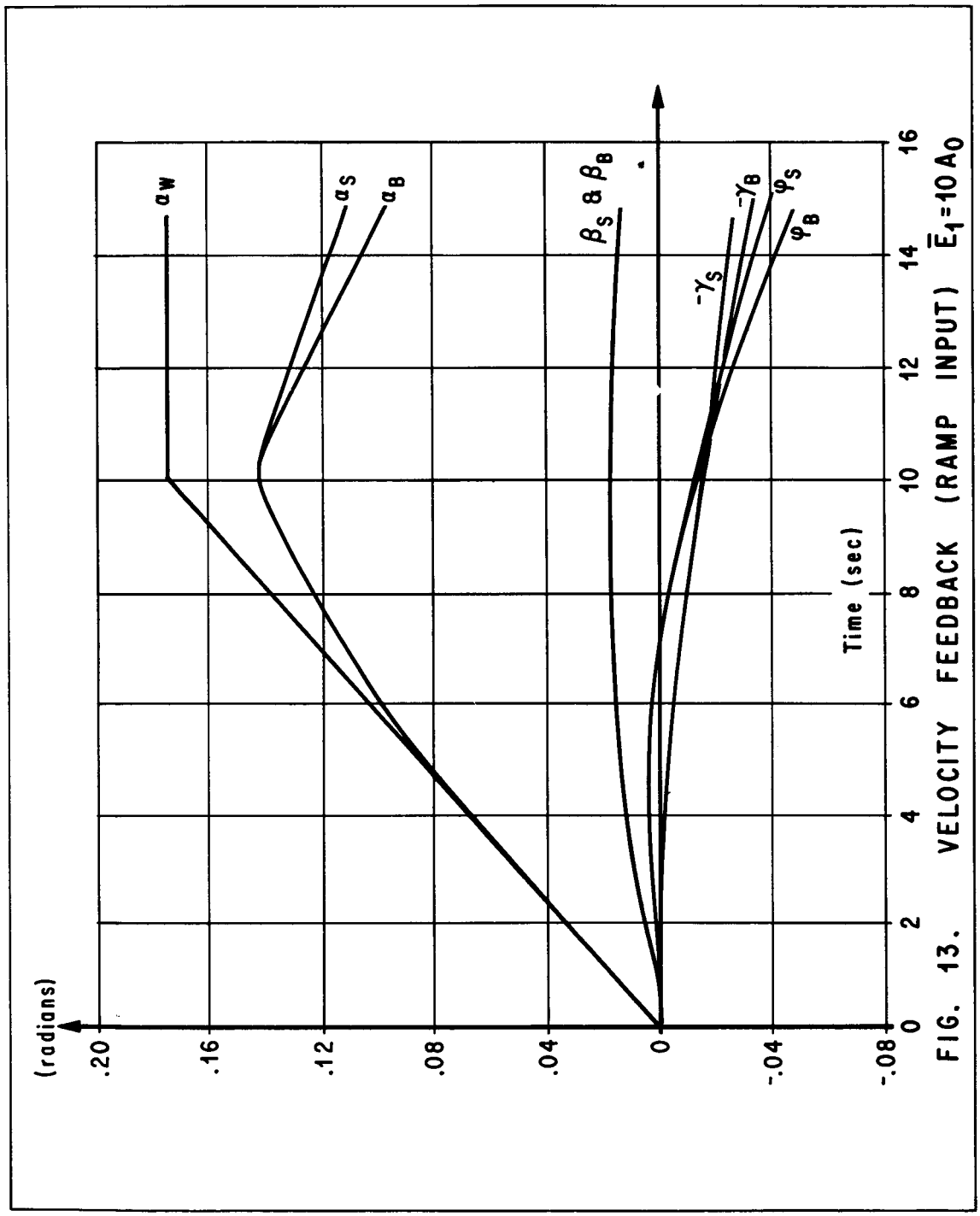


FIG. 13. VELOCITY FEEDBACK (RAMP INPUT) $\bar{E}_1=10A_0$

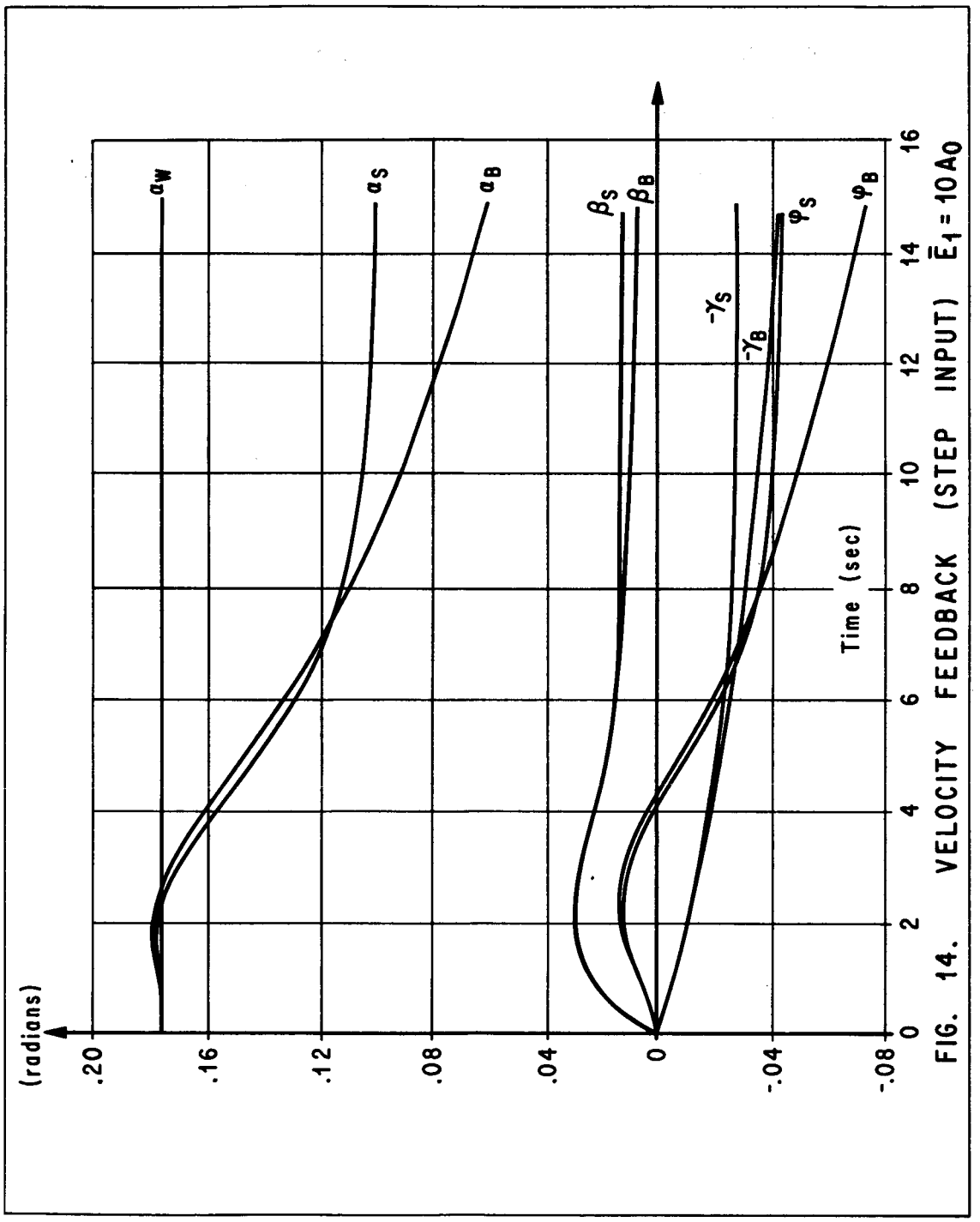


FIG. 14. VELOCITY FEEDBACK (STEP INPUT) $\bar{E}_1 = 10A_0$

## REFERENCES


1. Ryan, R., F. Swift, and D. Townsend, "A Simple Method for Determining the Bending Moment Equation," NASA TM X-53189, Aero-Astro. Research Review No. 1, October 1, 1964, Unclassified.

2. Hoelker, R. F., "The Principle of Artificial Stabilization of Aerodynamically Unstable Missiles," ABMA DA-TR-64-59.

3. Geissler, E. D., "Problems in Attitude Stabilization of Large Guided Missiles," ABMA DA-TR-21-60.

4. Hoelker, R. F., "Theory of Artificial Stabilization of Missiles and Space Vehicles with Exposition of Four Control Principles," NASA TN D-555, June 1961.

# THE ALLEVIATION OF AERODYNAMIC LOADS ON RIGID SPACE VEHICLES

By Mario H. Rheinfurth

The information in this report has been reviewed for security classification. Review of any information concerning Department of Defense or Atomic Energy Commission programs has been made by the MSFC Security Classification Officer. This report, in its entirety, has been determined to be unclassified.

This document has also been reviewed and approved for technical accuracy.

Helmut J. Horn
Chief, Dynamics and Flight Mechanics Division

E. D. Geissler
Director, Aero-Astrodynamics Laboratory

DISTRIBUTION

DEP-T

R-AERO

Dr. Geissler
Mr. Jean
Mr. Cummings
Mr. Horn
Mr. Bugg
Mrs. Chandler
Mr. Dahm
Mr. Reed
Mr. Rheinfurth (10)
Mr. Swift (10)
Miss Hopkins
Mr. Golmon
Mr. Stone
Mr. Baker
Mr. Lindberg
Mr. Kiefling
Mr. Lovingood
Mr. Pack
Mr. Verderaime
Mr. Worley
Mr. Milner
Mr. Buchanan
Mr. Townsend
Mr. Billups
Mr. Hammer
Mrs. King
Mr. Scherer
Mr. Ryan
Mr. Teuber
Mr. Hagood
Dr. Liu
Dr. McDonough
Mr. Wood
Mr. Hall
Mr. Brady
Mr. Mowery
Mr. B. G. Davis

R-AERO (Cont'd)

Mr. Cremin
Mr. W. Vaughan
Mr. R. Lewis
Dr. H. Krause

R-ASTR

Dr. Haeussermann
Mr. Hosenthien
Mr. B. Moore
Mr. Justice
Mr. Blackstone
Mr. Mink
Mrs. Fisher

R-P&VE

Dr. Lucas
Mr. Hellebrand
Mr. Hunt
Mr. Bullock
Mr. Showers

MS-T (6)

MS-IP

MS-IL (8)

MS-H

I-RM-M

CC-P

Scientific & Technical Information (25)
Center
Box 33, College Park, Maryland
ATTN: NASA Representative (S-AK/RKT)